

Origins of Intermediate Velocity Particle Production in Heavy Ion Reactions

L. Gingras¹, A. Chernomoretz², Y. Larochelle^{1*}, Z.Y. He^{1†}, L. Beaulieu¹, G.C. Ball^{3‡}, F. Grenier¹, D. Horn³, R. Roy¹, M. Samri⁴, C. St-Pierre¹, D. Thériault¹ and S. Turbide¹

¹ *Laboratoire de Physique Nucléaire, Département de Physique, Université Laval, Québec, QC, Canada G1K 7P4.*

² *Departamento de Física, Universidad de Buenos Aires, Buenos Aires, Argentina.*

³ *AECL, Chalk River Laboratories, Chalk River, ON, Canada K0J 1J0.*

⁴ *Laboratoire de Physique Nucléaire et Applications, Département de Physique, Université Ibn Tofail, Kénitra, Morocco.*

(October 25, 2018)

Investigation of intermediate-velocity particle production is performed on entrance channel mass asymmetric collisions of $^{58}\text{Ni}+\text{C}$ and $^{58}\text{Ni}+\text{Au}$ at 34.5 MeV/nucleon. Distinctions between prompt pre-equilibrium ejections, multiple neck ruptures and an alternative phenomenon of delayed aligned asymmetric breakup is achieved using source reconstructed correlation observables and time-based cluster recognition in molecular dynamics simulations.

PACS number(s): 25.70 -z, 25.70.Lm, 25.70.Mn, 25.70.Pq

During the last decade, reaction mechanisms studies of heavy ion collisions in the Fermi energy domain have unraveled new and interesting phenomena that can have major consequences on our understanding of both nuclear dynamics and excited nuclear matter properties. It was first established that binary dissipative collisions dominate the reaction cross section in this energy range for a large domain of entrance channel masses and asymmetries [1–5]. Early, it has been noticed that unlike the lower energy case, where exclusively two primary fragments (or one fusion fragment) are formed [6], the intermediate energy heavy ion collisions produce exotic structures that populate the intermediate-velocity (IV) zone between the two main collision partners [8–16]. This production of particles and fragments at mid-velocity is usually explained as the onset of the participant-spectator model of relativistic energies [17]. However, in the Fermi energy domain, the interplay between two-body interactions and collective motions from the nuclear mean field modifies this simple picture and can potentially give rise to peculiar mechanisms leading to such an important observed IV particle production. Of those mechanisms, fast light particles and coalescence clusters ejected by nucleon-nucleon collisions and multiple neck ruptures are usually expected to be responsible for the main IV particle production.

In this paper, we report for the first time clear distinctions between these prompt processes and an alternative phenomenon of delayed aligned asymmetric breakup that populates the intermediate-velocity zone by a deformation rupture of mainly the heavier of the colliding partners in mass asymmetric collisions. These distinctions were observed experimentally with intermediate-velocity particle correlation analysis of Ni+C and Ni+Au reactions at 34.5 MeV/nucleon.

A beam of ^{58}Ni accelerated at 34.5 MeV/nucleon by the coupled Tandem and Superconducting Cyclotron accelerators of AECL at Chalk River bombarded alternatively a 2.4 mg/cm² carbon target and a 2.7 mg/cm² gold target. Charged particles issued from these reactions were detected in the CRL-Laval 4π array constituted by 144 detectors set in ten rings concentric to the beam axis and covering polar angles between 3.3° and 140° . The first forward four rings (3.3° to 24°) are each made of 16 plastic phoswich detectors with energy detection thresholds of 7.5 (27.5) MeV/nucleon for element identification of $Z=1$ (28) particles. Between 24° and 46° , two rings of 16 CsI(Tl) crystals achieve isotopic resolution for $Z=1$ and 2 ions and element identification for $Z=3$ and 4 ions with energy thresholds ranging from 2 to 5 MeV/nucleon. The Miniball forms the last four rings (46° to 87° and 93° to 140°) and is constituted by PIN diode backed CsI(Tl) crystal detectors set in groups of 12 per ring. See [18] and references therein for more information on detectors and energy calibration. The main trigger for event recording was a charged particle multiplicity of at least 3 particles. The present work is restricted to events selected in the off-line analysis by a total detected charge of at least 31 units. This ensures good reconstruction of the quasi-projectile and IV particles characteristics.

In order to evaluate properties of the IV material, it needs to be isolated from its surrounding. This is done by reconstructing on an event-by-event basis the quasi-projectile (QP) and quasi-target (QT) emitters using a probabilistic reconstruction algorithm for the first nucleus and angular and velocity cuts for emissions of the second one. The statistical quasi-projectile reconstruction algorithm proceeds by two steps consisting in building probability tables for the attribution to the QP of a final detected particle and an application of these probabilities on an event-by-event basis. The main hypotheses on which the algorithm relies on are: (1) the event

*Present address: Joint Institute for Heavy Ion Research, Holifield Radioactive Ion Beam Facility, Oak Ridge, Tennessee 37831-6374.

†Present address: EXFO, 465 avenue Godin, Vanier, QC, Canada G1M 3G7.

‡Present address: TRIUMF, 4004 Wesbrook Mall, Vancouver, B.C., Canada, V6T 2A3

heaviest particle is assumed to be the QP evaporation residue, (2) particles emitted by the QP are isotropically distributed around this residue, and (3) the forward emission hemisphere of the QP is negligeably contaminated by emissions from other processes. Clearly, these hypotheses can only be verified in peripheral to semi-central collisions where the QP and QT are well enough separated in velocity space. Elements of the probability tables are referenced by classes of experimental impact parameters (b_{exp}), residue (Z_{res}) and emitted particle (Z_p) atomic numbers, as well as relative velocity between them (V_{rel}) and its absolute projection along the residue velocity in the CM (V_{rel}^{\parallel}). The experimental impact parameter was determined using a combination of two observables that are both closely related to the true impact parameter according to molecular dynamics and deep inelastic simulations [19]. These observables are the total parallel momentum of all charged particles in the forward velocity hemisphere of the center of mass (CM) reference frame (Π_{\parallel}^{cm}) and the anisotropy ratio of light charged particles ($Z \leq 2$) in that same frame (R_A) [20].

$$b_{exp} = r_0(A_P^{1/3} + A_T^{1/3}) \frac{1 + \frac{\Pi_{\parallel}^{cm}}{P_P^{cm}} - c \frac{tg^{-1}(R_A)}{\pi/2}}{2}, \quad (1)$$

where A_P , A_T and P_P^{cm} are respectively the projectile mass number, target mass number and projectile CM momentum. $r_0 = 1.2 fm$ and the constant c was experimentally adjusted to 1.2. Following hypotheses (2) and (3), the QP attribution probability for particles emitted in the forward hemisphere is fixed at unity, whereas the probability for the backward-emitted ones is determined by dividing the forward with the backward relative velocity spectra gated by b_{exp} , Z_{res} , Z_p and V_{rel}^{\parallel} . Details and results of this method for QP properties can be found in refs. [18,21,22]. Particles detected in the Miniball were attributed to the QT emitter as well as particles having parallel velocity along the residue direction of less than $-0.12c$. All remaining final particles are assigned to the IV component.

Figure 1 shows the evolution with experimental impact parameter of the parallel velocity distribution in the CM reference frame of the reaction charged products according to their attributed origin. In both reactions, as the impact parameter decreases, the mean parallel velocity of the QP products also decreases, reflecting the energy damping of the projectile. Along with this obvious effect, particle production from the QT and IV material, for $^{58}\text{Ni}+\text{Au}$ reaction, becomes more important as the collision gets more violent. In the case of $^{58}\text{Ni}+\text{C}$ reaction, the α particle sub-structure of the ^{12}C target makes it easy to break at all detected impact parameters. Particle production in the IV region appears also to be strong on the whole b_{exp} range. With the decrease of impact parameter, the average velocity of the IV charged products in the $^{58}\text{Ni}+\text{C}$ system increases above v_{NN} , whereas for $^{58}\text{Ni}+\text{Au}$ system, it stays close to it on the whole range,

with a small tendency to decrease toward the QT velocity.

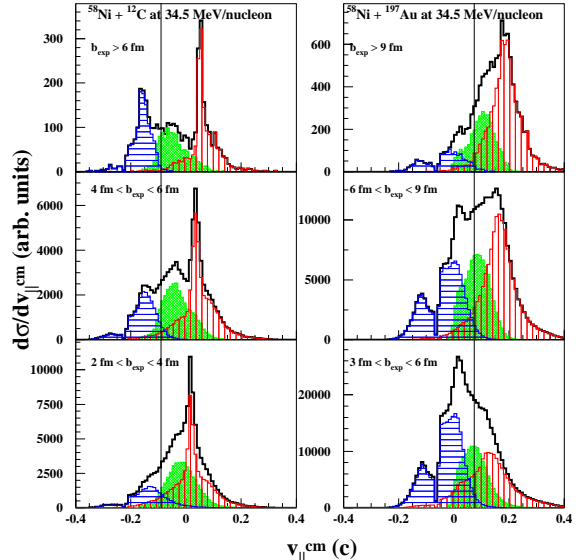


FIG. 1. CM Parallel velocity distributions for charged particles of $^{58}\text{Ni}+\text{C}$ (left) and $^{58}\text{Ni}+\text{Au}$ (right) reactions. The total distributions (thick solid lines) are broken in QP (vertical hatches), QT (horizontal hatches) and IV (shaded histogram) contributions. The vertical line shows v_{NN} .

In order to get information on the time formation and characteristics of the IV material produced in these mass asymmetric heavy ion reactions, molecular dynamics simulations were performed. A semi-classical molecular dynamics model with a spherical two-body interaction potential presenting realistic nucleon-nucleon cross sections and including Coulomb interactions has been used to modelize semi-peripheral reactions of the $^{58}\text{Ni}+^{12}\text{C}$ and $^{58}\text{Ni}+^{197}\text{Au}$ systems at 34.5 MeV/nucleon. Focusing on the nucleon-nucleon correlations that give rise to the fragment formation processes, a clusterization algorithm making use of the ‘minimum spanning tree in energy space’ (MSTE) criterion, has been used. Right after the most violent stage of the collision, an MSTe cluster recognition step allowed us to sort the particles as belonging to the projectile-like fragment (PLF), the target-like fragment (TLF), or as prompt emitted particles (PEP) not spatially correlated neither to the PLF nor the TLF. The time at which every asymptotic cluster have actually been emitted (t_e) can be calculated within the model by simply tracing back the dynamical evolution of the reaction. See [23] and refs. therein for more specific details about the model used and the cluster time origin analysis of mass asymmetric reactions.

The extracted emission times for particles originating from the PLF, TLF and PEP components were used to put into evidence the origins of different regions of the asymptotic velocity space. Parallel velocity spectra of

particles originating from these components were separated in figure 2 according to their calculated emission time. From panels (a)-(c), it can be seen that for the $^{58}\text{Ni}+^{197}\text{Au}$ system, the IV region is populated not only by PEP particles but also by a supplementary contribution coming mainly from the heavier partner of the reaction. Moreover, a different time scale can be associated with each kind of contribution. The PEP are mainly light clusters ($Z \leq 5$) that were configurationally well differentiated from the PLF and TLF very early in the evolution. On the other hand (see panels (e),(i),(m)), the target-like intermediate-velocity clusters were spatially linked to the TLF at PLF-TLF separation time and were emitted later in the evolution, mainly between 150 fm/c and 500 fm/c. For the $^{58}\text{Ni}+^{12}\text{C}$ case (fourth column of fig. 2), an important contribution to the IV emission coming now from the PLF can also be recognized. Again, that contribution is not a prompt one, but takes place in the same mid-range temporal interval than the one observed in the other reaction.

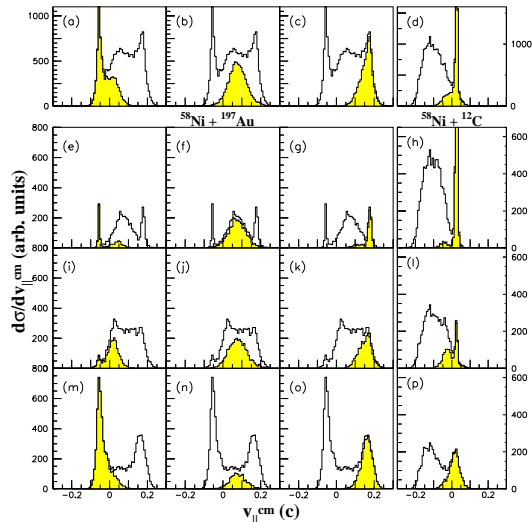


FIG. 2. Histograms of $v_{||}^{cm}$ asymptotic distributions. In the first, second and third columns, the contributions of the TLF, PEP, and PLF emissions have been selectively shadowed for the $^{58}\text{Ni}+^{197}\text{Au}$ reaction ($7\text{fm} \leq b \leq 8\text{fm}$). The fourth column shows the respective calculation for the $^{58}\text{Ni}+^{12}\text{C}$ reaction ($3\text{fm} \leq b \leq 4.5\text{fm}$) shadowing the PLF emissions. Figs. (a)-(d) show total distributions. In Figs. (e)-(h), (i)-(l), and (m)-(p) the contribution of particles with emission times of $t_e < 150$ fm/c, $150 \text{ fm/c} \leq t_e < 500$ fm/c, and $t_e \geq 500$ fm/c after the collision are shown respectively.

These findings suggest two scenarios for the origin of IV particles. On one hand, the prompt emission at the highly collisional stage of the reaction of mainly PEP. On the other, a mechanism where a dynamical deformation of the heavy partner of the reaction develops, eventually leading to a scission followed by a Coulombian push that projects the emitted particles towards the intermediate-velocity range, this second alternative

occurring on a longer time scale.

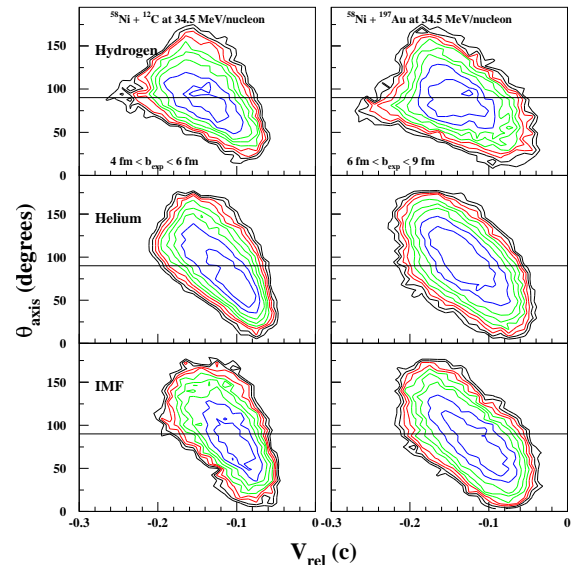


FIG. 3. θ_{axis} vs V_{rel} logarithmic contour plots for IV attributed particles in the $^{58}\text{Ni}+\text{C}$ (left) and $^{58}\text{Ni}+\text{Au}$ (right) systems for two specific ranges of b_{exp} .

To investigate these possible origins of IV particles in the data, a study has been done of the angular relations between their emission direction (evaluated from their velocity vector in the reconstructed center of mass of all IV particles in the event) and the reaction axis, defined by the direction of the velocity vector of the reconstructed QP in the system CM reference frame. Figure 3 shows the distribution of the angle between those two vectors as a function of the relative velocity between the IV particle and the QP residue, for particles attributed to the IV component. Hydrogen, Helium and IMF ($Z = 3 - 7$) contributions are shown on the figure. From collisions of the $^{58}\text{Ni}+\text{Au}$ system, it is possible to notice firstly the nearly forward-backward symmetry of the distributions around $\theta_{axis} = 90^\circ$ for hydrogens up to IMF's, as well as a sizeable focusing of $Z = 1$ particles at 90° . This can be understood as a fast emission of particles and excited clusters from the overlapping nuclear matter. Excited clusters will decay on a variable time scale and most of the final products will be released in an almost field free region, therefore with isotropic angular distribution. However, the prompt ejected particles following early nucleon-nucleon collisions in the overlap region will be subject to the Coulomb field of the two heavy nuclei as well as to blocking from the saturated quantum phase space regions. These particles will therefore be predominantly emitted on a plane perpendicular to the reaction axis. In the $^{58}\text{Ni}+\text{C}$ reaction, forward-backward symmetry around $\theta_{axis} = 90^\circ$ is destroyed, as can be seen from the left panels of figure 3. Along with a narrower distribution, an enhancement of forward directed IV par-

ticles with small relative velocity with the QP residue is observed for $Z = 2$ particles and IMF's. This could be a signature for the presence of a supplementary process that populates the IV region from an asymmetric and aligned breakup of the QP. This production process of IV particles seems to be less dominant in the $^{58}\text{Ni}+\text{Au}$ reaction since no such enhancement is observed. These experimental results go along the molecular dynamics predictions that aligned asymmetric breakup occurs mainly on the heavier partner side of the IV region [23]. The fact that the effect is not experimentally seen on the QT side of the $^{58}\text{Ni}+\text{Au}$ system is just a result of inadequate detection thresholds for particles in this region.

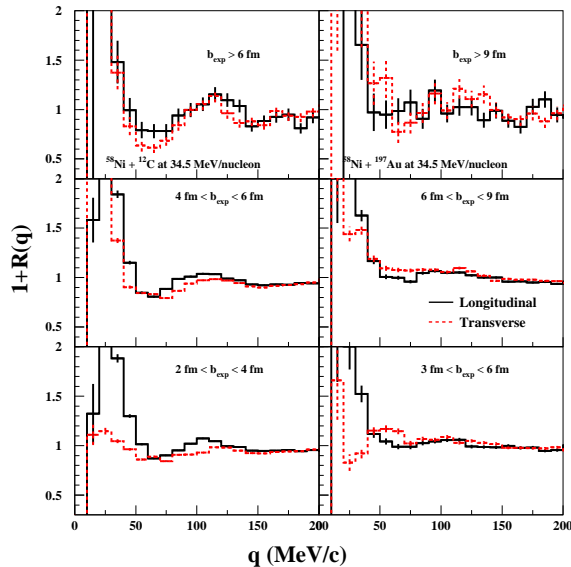


FIG. 4. $\alpha - \alpha$ correlation functions broken in longitudinal (solid line) and transverse (dashed line) contributions for IV attributed particles in the $^{58}\text{Ni}+\text{C}$ (left) and $^{58}\text{Ni}+\text{Au}$ (right) systems.

Origins of IV particles have been studied further by two-particle correlation functions with directional cuts. A similar method was originally used for proton-proton [24,25] and IMF-IMF [26] correlation functions in order to probe the space-time extent of a compound source in central collisions. In our case, α particles have been chosen for this study for their abundance in the IV region and for the reason that the first unstable excited state of the two- α particles decaying ^8Be nucleus has a lifetime of about 130 fm/c ($\Gamma \approx 1.5$ MeV), which is about the time it takes to the aligned asymmetric breakup process to take place. The experimental $\alpha - \alpha$ correlation function is defined as

$$1 + R(q) = \frac{N_{\text{coinc}}(q)}{N_{\text{back}}(q)}, \quad (2)$$

where $N_{\text{coinc}}(q)$ is the coincident α pairs yield with relative momentum q and where $N_{\text{back}}(q)$ is the background

yield constructed by means of a modified event-mixing technique for IV attributed particles. Since final particles in each event have their velocity vectors related to the reaction axis, a strict application of the standard event-mixing technique introduces unreal contributions in the background yield for pair of events with different reaction axis directions. Therefore, by taking advantage of the cylindrical symmetry of the detector apparatus, an improved event-mixing technique was used which involved a rotation of the second event of a background pair in the plane perpendicular to the beam, so as to make coincide the ϕ angle of the two event reaction axis. Correlation functions constructed with this technique were measured for two directional cuts in the emission direction of the two α particles relative to the momentum direction of the pair in the QP reference frame. Longitudinal correlation functions stand for angles between the two directions ranging from 0° up to 60° , whereas transverse correlation functions refer to angles from 60° to 90° . Figure 4 shows these correlation functions for the two studied systems and for different impact parameters. From the figure, the ground state and the first excited state of the particle unstable ^8Be nucleus are clearly seen at relative momenta of 25 and 100 MeV/c respectively. The weaker transverse correlation function for the ^8Be ground state at low b_{exp} was expected from simple Coulomb trajectory calculations including ^8Be decay and average experimental velocity space relations for QP and IV particles. It is due to the small relative angle between the emitted α particles in the laboratory reference frame and to the non-negligible size of the detectors leading to double hits that are discriminated out of the correlation function analysis. However, the calculation showed that multiple hits contribute to a negligible amount in the difference between longitudinal and transverse breakup for the first excited state decay in the IV region.

The approximately equal strengths observed for the longitudinal and transverse correlation functions in the first excited state region of interest ($80 < q < 120 \text{ MeV}/c$) of the $^{58}\text{Ni}+\text{Au}$ reaction emphasize that ^8Be resonances in the IV region bears no alignment relations with the QP and are therefore probably isolated from it in space-time at the point of their breakup. This can be understood as the fast QP leaves the interaction region very early without dragging nuclear material that can be pushed back in the IV region later on. However, differences between the strengths of first excited state transverse and longitudinal correlation functions are observed in the $^{58}\text{Ni}+\text{C}$ reaction for collisions of experimental impact parameter below 6 fm . The Coulomb trajectory calculation of a system, composed initially of a ^{58}Ni QP emitting from its surface a ^8Be nucleus in its first excited state, has shown that tidal forces were strong enough to flip about 50% of initially emitted longitudinal α pairs in final transverse ones, whereas only 5% of the reverse case occur. This effect expected for isotropic α particle decay from ^8Be in the field of the remaining QP is however not observed experimentally. On the

contrary, longitudinal decay appears to be dominant in mid-peripheral reactions. Therefore, this experimentally observed stronger longitudinal correlation function tends to imply an important initial polarization in the emission of first excited state ${}^8\text{Be}$ resonances in the longitudinal direction. This can possibly occur from a deformation of the QP in the reaction axis direction, thus constraining alignment conditions for the ${}^8\text{Be}$ resonance formation. In mid-peripheral reactions, these more important deformations will lead the QP to a breakup configuration that will ultimately push back some of the material in the IV region.

This deformation breakup effect populating the IV region with light fragment and particles is associated to the delayed aligned asymmetric breakup observed in the molecular dynamics simulation [23] and in the experimental θ_{axis} distributions for the ${}^{58}\text{Ni}+\text{C}$ system. More important deformations are therefore expected on the heavier partner side in a mass asymmetric heavy ion reaction. This can be a result of the different surface boundary conditions at the two poles of the reseparating system. An asymmetrically shaped neck will breakup earlier on the lighter partner side and will stay attached to the heavier partner for a longer time, potentially leading it to breakup in a delayed aligned asymmetric fashion.

In conclusion, we have demonstrated in this paper the existence of two mainly different origins for intermediate-velocity particle and fragment production. The use of a source reconstruction technique has permitted to study on an event-by-event basis the characteristic angular emission pattern of the IV particles as well as their relation with the remaining QP in two-particle correlations. Important differences between two entrance channel mass asymmetric reactions were observed on the QP side of the intermediate-velocity space. With help of time-based cluster recognition algorithm applied to molecular dynamics simulation [23], it has been possible to determine the time scales associated to two different phenomena. The first origin is related to prompt nucleon-nucleon collisions that occur in the overlap zone of the two colliding nuclei. These processes will eject light particles and excited clusters out of the overlap on a very short time scale of the order of the reseparation time. Excited clusters ejected at this stage will however emit particles on a longer time scale. The second origin of IV particle production is related to the collective motion of nucleons at the perturbed ends of the QP and QT. Important deformations will be carried by the heavier partner of the collision and will lead it to a mass asymmetric breakup aligned along the reseparation axis. This is expected to happen after a delay of the order of 150-500 fm/c. In entrance channel mass symmetric collisions, molecular dynamics calculations predict this second origin of IV particles to happen on both QP and QT. Recent results for the heavier system ${}^{116}\text{Sn}+{}^{93}\text{Nb}$ at 29.5 MeV/nucleon presenting the necessity of adding a surface emission component to the neck component at mid-velocity are compatible with this expectation [27]. It can also be noted that

the phenomenon of delayed aligned asymmetric breakup is potentially related to previously observed processes of dynamical projectile splitting [29] and fast asymmetric fission [30] at lower bombarding energies. It will be interesting in future analysis and experiments to study the isospin dependence of the IV products according to their specific origin, in order to disentangle shape, thermal and chemical equilibration processes. In fact, a possible chemical motion in reaction to the slow surface/volume deformations involved in the delayed aligned asymmetric breakup mechanism could explain in part the observation of higher N/Z ratio of mid-rapidity IMF's relative to total systems with no initial neutron enrichment [28].

ACKNOWLEDGMENTS

This work has been supported in part by the NSERC, FCAR, University of Buenos Aires and CONICET.

-
- [1] B. Lott *et al.*, Phys. Rev. Lett. **68**, 3141 (1992).
 - [2] J.F. Locolley *et al.*, Phys. Lett. **B325**, 317 (1994).
 - [3] J. Péter *et al.*, Nucl. Phys. **A593**, 95 (1995).
 - [4] Y. Larochelle *et al.*, Phys. Lett. **B352**, 8 (1995).
 - [5] L. Beaulieu *et al.*, Phys. Rev. Lett. **77**, 462 (1996).
 - [6] W.U. Schröder and J.R. Huizenga, "Damped nuclear reactions", published in "Treatise on heavy-ion science Vol. 2", Ed. D.A. Bromley, Plenum Press (1984).
 - [7] D.R. Bowman *et al.*, Phys. Rev. Lett. **70**, 3534 (1993).
 - [8] C.P. Montoya *et al.*, Phys. Rev. Lett. **73**, 3070 (1994).
 - [9] J.F. Locolley *et al.*, Phys. Lett. **B354**, 202 (1995).
 - [10] J. Töke *et al.*, Phys. Rev. Lett. **75**, 2920 (1995).
 - [11] J.F. Dempsey *et al.*, Phys. Rev. C **54**, 1710 (1996).
 - [12] Y. Larochelle *et al.*, Phys. Rev. C **55**, 1869 (1997).
 - [13] J. Lukasik *et al.*, Phys. Rev. C **55**, 1906 (1997).
 - [14] T. Lefort *et al.*, Nucl. Phys. **A662**, 397 (2000).
 - [15] E. Plagnol *et al.*, Phys. Rev. C **61**, 014606 (2000).
 - [16] G. Poggi *et al.*, Nucl. Phys. **A685**, 296c (2001).
 - [17] G.D. Westfall *et al.*, Phys. Rev. Lett. **37**, 1202 (1976).
 - [18] L. Gingras, M.Sc. Thesis, Université Laval (1998).
 - [19] L. Tassan-Got *et al.*, Nucl. Phys. **A524**, 121 (1991).
 - [20] H. Ströbele, Phys. Rev. C **27**, 1349 (1983).
 - [21] L. Gingras *et al.*, in Proceedings of the XXXVIth Winter Meeting on Nuclear Physics, Bormio, Italy, edited by I. Iori, p361 (1998).
 - [22] Z.Y. He *et al.*, Phys. Rev. C **63**, 011601(R) (2000).
 - [23] A. Chernomoretz *et al.*, arXiv:nucl-th/0108072, (2001).
 - [24] M.A. Lisa *et al.*, Phys. Rev. Lett. **71**, 2863 (1993).
 - [25] M.A. Lisa *et al.*, Phys. Rev. C **49**, 2788 (1994).
 - [26] T. Glasmacher *et al.*, Phys. Rev. C **50**, 952 (1994).
 - [27] S. Piantelli *et al.*, arXiv:nucl-ex/0105004, (2001).
 - [28] Y. Larochelle *et al.*, Phys. Rev. C **62**, 051602(R) (2000).
 - [29] A. Olmi *et al.*, Phys. Rev. Lett **44**, 383 (1980).
 - [30] G. Casini *et al.*, Phys. Rev. Lett **71**, 2567 (1993).